Ubanozie Julian Obibuike[1], Stanley Toochukwu Ekwueme[1], Nnaemeka Princewill Ohia[2], Frank Chinedu Ukaeru[1], Ifeanyi Michael Onyejekwe[1], Mathew Chidubem Udechukwu[1]

[1]Department of Petroleum Engineering, Federal University of Technology, Owerri, Nigeria, [2]Africa Centre of Excellence in Future Energies and Electrochemical Systems (ACE-FUELS), Owerri, Nigeria

Scientific paper
ISSN 0351-9465, E-ISSN 2466-2585
https://doi.org/10.62638/ZasMat1329

Zastita Materijala 67 (1)
14 - 35 (2026)

Modelling and optimisation of geothermal binary ORC systems using response surface methodology and artificial neural networks

ABSTRACT

This study focuses on the modeling and optimization of geothermal binary Organic Rankine Cycle (ORC) systems to enhance power generation from geothermal systems using water as geofluid. Aspen HYSYS, utilizing the Peng-Robinson property package, was used to simulate the process, generating critical process data for subsequent modeling and optimization. Response Surface Methodology (RSM) and an Artificial Neural Network (ANN) were employed to model the relationships between input factors and output response, utilizing a Box-Behnken Design (BBD) for three key input variables: working fluid flow rate, working fluid outlet pressure, and turbine outlet pressure. Both RSM and ANN demonstrated strong predictive capabilities, with RSM achieving an R2 value of 0.9966 and an RMSE of 12.254, while ANN achieved an R2 value of 0.9886 and an RMSE of 23.722, indicating that RSM marginally outperformed ANN in terms of modelling accuracy. Optimization of the ORC system was conducted using RSM and ANN coupled with a Genetic Algorithm (ANN-GA), aimed at determining the optimal values for input and output parameters. The ANN-GA optimization results were validated using Aspen HYSYS and showed superior performance over RSM. ANN-GA predicted optimal values of working fluid flow rate, working fluid outlet pressure, and turbine outlet pressure as 12 kg/s, 19 bar, and 1.2 bar, respectively, which perfectly matched the Aspen HYSYS validation results. This optimization yielded a power output of 958.48 kW, which closely aligned with the Aspen HYSYS validation output of 952.9 kW, reflecting a minimal percentage error of 0.59%. Conversely, RSM predicted slightly deviated optimal values of 11.8 kg/s, 18.47 bar, and 1.2 bar, with a corresponding power output of 940.78 kW. When validated with HYSYS, the RSM-predicted output was 927.2 kW, resulting in a higher percentage error of 1.46%, thereby underperforming relative to ANN-GA. The study highlights the comparative strengths of RSM and ANN-GA, demonstrating that while RSM excels in accurately modeling the relationship and interactions between input factors and output responses, the ANN-GA framework exhibits a significantly higher capability in navigating complex nonlinear optimization landscapes. This highlights the effectiveness of integrating machine learning models with meta-heuristic algorithms for enhanced optimization performance. The findings contribute to advancing the methodology for optimizing geothermal ORC systems and offer a robust framework for improving power generation efficiency in geothermal energy applications.

***Keywords**: Geothermal energy, RSM, ANN, genetic algorithm, Hysys simulation, Power generation, binary ORC systems*

1. INTRODUCTION

The global reduction of fossil fuel resources and the need to mitigate carbon emissions are critical challenges faced worldwide. Despite these, energy demand continues to rise, necessitating alternative energy solutions to meet global requirements. Geothermal energy is a promising solution due to its abundance, eco-friendliness, and renewable nature [1, 2].

As a clean energy resource, geothermal energy offers numerous advantages over other renewable sources, including its higher reliability, sustainability, and capacity factor. It is less affected by climatic conditions, making it a reliable source of energy, particularly in regions with geothermal reserves.

Geothermal energy is derived from the Earth's subsurface, with temperatures ranging from 50°C to 350°C [3]. Geothermal resources can be classified into four main groups: hydrothermal, magma, hot-dry rock, and geo-pressured [4]. Among these, hydrothermal resources are the most commonly utilized, existing in either vapor-dominated or liquid-dominated forms, depending

*Corresponding author: Stanley ToochukwuEkwueme
E-mail: stanleyekwueme@yahoo.com
Paper received: 25.12.2024.
Paper corrected: 30.04. 2025.
Paper accepted: 09. 06.2025.

on geological conditions. Vapor-dominated systems typically exhibit temperatures between 250°C and 300°C and produce superheated (dry) steam [5]. In contrast, liquid-dominated systems can generate wet steam or water, making them versatile in energy production [5, 6].

The utilization of geothermal energy for power generation is divided into two main categories: power generation systems and reinjection facilities (or alternative solutions for non-condensable gases) [7]. The former includes the production well and closed power cycle, while the latter deals with compressor trains and reinjection wells [8]. Geothermal power plants are a key method for harnessing geothermal energy and fall into three main types: dry-steam, flash, and binary [9]. Each technology is suitable for different temperature ranges. Dry-steam and flash systems are used for high-temperature sources (above 180°C), while binary plants are employed for lower temperature resources (below 180°C).

Globally, dry-steam, flash, and binary technologies account for approximately 26%, 58%, and 15% of the market, respectively, with emerging technologies making up about 1% of facilities [1]. However, binary plants are becoming increasingly popular due to their flexibility in utilizing low-to-medium-temperature resources. In fact, over 270 binary power plants are currently operational worldwide [10].

In a dry-steam geothermal system, high-temperature and high-pressure steam is directly extracted from underground and expanded through a steam turbine to drive an electricity generator [8]. Wet-steam geothermal systems, on the other hand, involve separating the wet steam into saturated steam and geothermal water ([11]. The saturated steam is expanded through a turbine to generate electricity, while the geothermal water can be flashed at lower pressure to produce additional steam, which is also used for power generation. This configuration allows for efficient use of geothermal resources, particularly in areas where wet-steam conditions prevail.

While the traditional Rankine cycle using water as a working fluid is widely used for power generation, it is not always suitable for low- and medium-temperature geothermal resources. The boiling point of water is often too high for these resources, leading to inefficiencies [10]. Additionally, using steam cycles can result in issues such as turbine blade erosion, condensation during expansion, and the need for superheating, which complicates turbine design and increases costs. As a result, alternative cycles like the organic Rankine cycle (ORC), supercritical Rankine cycle, Kalina cycle, and flash cycle have been proposed for low-temperature heat conversion.

The ORC is particularly well-suited for low-to-medium-temperature geothermal applications due to its use of organic working fluids with lower boiling points than water. These organic fluids allow the ORC to utilize a wide range of heat sources [10]. The cycle operates similarly to the traditional Rankine cycle, where the working fluid is heated to boiling, and the resulting vapor drives a turbine that generates electricity. Afterward, the vapor is condensed back into a liquid and recirculated in the system.

Binary cycle technology, which includes ORC and Kalina cycles, is often used for liquid geothermal sources or medium-to-low-temperature resources (100–170°C) [1]. One of the key advantages of binary systems is their enclosed geothermal fluid loop, which prevents environmental pollution by reinjecting potentially harmful geothermal fluids back underground. In ORC-based binary geothermal power plants, the organic working fluids ensure system efficiency and environmental safety [12].

Despite the benefits, creating an efficient binary ORC system remains a significant challenge for the geothermal industry [13]. These systems require substantial capital investment, making proper planning and design essential. Research and development efforts focus on field tests, numerical modeling, simulation, and optimization to enhance system performance [1].

A successful binary ORC system must generate sufficient heat to produce electricity and maintain a production life of at least 30 years. Understanding and optimizing key parameters, including fluid properties, cycle efficiency, and resource characteristics, is crucial to improving system performance. By systematically testing various parameter combinations, engineers can design more efficient and cost-effective geothermal systems, thereby contributing to the global energy transition [14].

In optimization studies and experimental setups, process variables often depend on or interact with one another. Understanding the output-input relationships requires a deep comprehension of these interactions. Evaluating all possible combinations of parameters can be time-consuming, especially when running complex numerical simulations [13]. To address this challenge, numerical simulations are often used to study the effects of individual parameters, which are then used to design surrogate models. These models help streamline system development, reducing the time required for optimization while maintaining accuracy [14].

In the design of thermo-power generation blocks for binary Organic Rankine Cycle (ORC) systems using H_2O as the geothermal working fluid, various factors significantly influence performance, including cycle layout parameters, design specifications, and the variability of heat source and heat sink conditions [14]. Optimization of such systems is essential for maximizing efficiency and output, and the Response Surface Methodology (RSM) serves as a powerful and versatile tool for this purpose [15, 16]. RSM is a statistical and mathematical approach designed for constructing experimental models, analyzing variations in input factors, and generating a response surface that relates these variables to the desired output ([17]. By employing carefully structured experimental designs, such as Box-Behnken or Central Composite Designs, RSM facilitates the exploration of complex parameter spaces with high efficiency. This enables the identification of relationships between multiple input variables and the response variable, thereby allowing for simultaneous analysis and optimization [18].

The response surface generated by RSM provides a detailed map of how changes in input variables affect the system's output, making it a reliable method for identifying optimal ranges for key input parameters. This capability is particularly valuable in geothermal systems, where factors such as turbine inlet conditions, working fluid properties, and thermal efficiency must be fine-tuned to achieve maximum power output. RSM has been successfully applied in various studies to optimize and predict performance in ORC systems [18]. Its applications include turbine design optimization, where the geometry and operating conditions are adjusted for peak performance, and determining input parameters for maximizing thermal efficiency and output in geothermal power cycles [15]. By providing a systematic and statistically robust approach, RSM reduces the time and computational effort required for optimization while ensuring reliable and accurate predictions [17, 19].

Many scholars have investigated the use of RSM for modelling and optimisation of geothermal systems. Assareh et al. [18] employed RSM with Design-Expert software to optimize a geothermal-based energy system producing liquid hydrogen, cooling, hot water, and power. Using R123 as the working fluid, optimal exergy efficiency (43.91%) and cost rate (45.12 $/h) were determined. RSM effectively modeled and analyzed the impact of design variables, identifying Regina, Canada, as the optimal location based on performance and environmental benefits. Al Jubori et al. [20] employed RSM as part of a multi-objective optimization methodology integrating mean-line design, 3D CFD analysis, and ORC modeling for a small-scale radial-inflow turbine. Blade geometry was optimized using 20 design points, achieving 13.95% and 17.38% improvements in turbine and cycle thermal efficiencies, respectively. Kazemian et al. [21] utilized RSM with the central composite design to optimize input parameters for a combined GT/ORC/ARS system, demonstrating its superior economic performance over GT/ORC/GSHP systems. Sensitivity analysis further evaluated economic parameters like payback period and NPV. Azizi et al. [22] integrated RSM with grey wolf optimization for a geothermal-natural gas cogeneration system. Optimization achieved 45.2% exergy efficiency and a unit product cost of 3.82 $/GJ, highlighting RSM's role in enhancing performance and profitability.

In recent years, machine learning methods have revolutionized the optimization and performance enhancement of Organic Rankine Cycle (ORC)-based plants. Among these methods, Artificial Neural Networks (ANNs) have demonstrated exceptional capabilities in predicting, classifying, and approximating functions, particularly in handling complex and nonlinear relationships [23]. This has made ANNs an indispensable tool for solving real-world challenges across diverse applications, including shallow geothermal systems. ANNs, particularly those implementing backpropagation algorithms, have been pivotal in advancing geothermal energy operations, enhancing efficiency and sustainability [23]. The integration of machine learning techniques in ORC systems began with their application to predict and optimize system performance [24].

Tugcu and Arslan [25] applied a two-stage ANN model to optimize a geothermal absorption refrigeration system, analyzing 3660 designs with energy, exergy, and NPV metrics. ANN trained with backpropagation algorithms achieved error rates as low as 0.07%, effectively predicting and optimizing COP and exergy efficiency. Ziviani et al. [26] developed an ANN to predict performance in ORC experiments using scroll expanders, achieving high accuracy for turbine parameters like inlet pressure and rotation speed. Yilmaz and Koyuncu [27] modelled and optimized the Afyon Geothermal Power Plant using a multi-layer ANN with a genetic algorithm, achieving energy and exergy efficiencies of 10.4% and 29.7%. The optimized payback period and exergy cost were calculated as 2.87 years and $0.0176/kWh, respectively. Cetin et al. [28] modeled a binary geothermal power plant

(GPP) with ANN to optimize thermodynamic performance. By analyzing reference point data, the model estimated power output and exergy efficiency, determining the best parameter configurations for maximum performance. Yilmaz and Sen [29] utilized an ANN-based Genetic Algorithm (GA) to optimize a geothermal and solar-assisted energy and hydrogen production system under varying climatic and operational conditions. The ANN-GA model predicted power output and hydrogen production, achieving a cost of hydrogen at $1.576/kg and a unit electricity cost of $0.027/kWh.

Chanthamaly et al. [30] applied ANN classification algorithms to predict maintenance schedules for geothermal wells, achieving 99.83% accuracy using K-means clustering. The ANN-supported predictive maintenance ensured system reliability and minimized power loss. Xue et al. [23] proposed an ANN-Differential Evolution (DE) optimization framework for a three-horizontal-well EGS, achieving a low LCOE of $0.0376/kWh, with ANN models demonstrating high predictive accuracy ($R^2 > 0.996$) and significant time savings (36,000x faster than simulations). Hsieh et al. [31] trained an ANN using data from a 3D axial turbo-expander model to predict key cycle parameters under off-design conditions, enabling long-term performance analysis for geothermal fields. Zhou et al. [32] Introduced a hybrid framework combining ANN with mathematical programming to optimize ORCs, achieving high classification (99% accuracy) and regression (mean errors <1%) performance. The mixed-integer linear programming (MILP) approach significantly reduced computational time while optimizing net exergy to 28.66 MW.

Chitgar et al. [33] used ANN-GA for multi-objective optimization of geothermal-based desalination systems, identifying configurations that improved power generation by 150% and water production by 60%, while evaluating optimal working fluid combinations under different temperatures. Shakibi et al. [34] evaluated ANN algorithms for optimizing geothermal-hydrogen systems in Australia, achieving a 46.27% exergy efficiency, 1.84-year payback, and high accuracy (mean absolute error: 2.28×10^{-14}) in predicting system performance under multi-objective scenarios. Ling et al. [35] developed an ANN-based prediction and optimization model for a binary cycle geothermal power plant. The model controlled working fluid circulation rates, optimizing net power production and reducing costs, outperforming traditional physics-based approaches. Farajollahi et al. [36] combined ANN with response surface methodology (RSM) for hybrid power plant optimization, using ANN to map independent variables to thermal efficiency and cost. The GA-based optimization identified parameters achieving a thermal efficiency of 30.47% and a levelized product cost of $13.04/GJ.

2. LITERATURE REVIEW

2.1.ORC Cycle Working Fluids

The performance of an ORC system is highly dependent on the choice of working fluid, making this selection a critical factor in system design and efficiency. Selecting the most suitable organic working fluid involves considering a variety of parameters, including thermodynamic properties, environmental impact, safety concerns, and economic factors. These criteria collectively influence the overall efficiency, cost, and sustainability of the ORC system [1].

From an environmental and safety perspective, working fluids must comply with strict regulations related to Global Warming Potential (GWP) and Ozone Depletion Potential (ODP). Fluids used in ORC systems should have a GWP below 150 and exhibit no ODP to minimize environmental harm, in line with global climate targets and environmental protection efforts [33]. Furthermore, the working fluids should also possess favourable safety characteristics, such as low flammability and toxicity. The careful selection of non-hazardous fluids helps to reduce operational risks and ensures compliance with safety regulations in industrial settings [37].

When choosing a working fluid, other critical factors include thermodynamic properties that directly affect the system's efficiency. Fluids with low specific volumes are preferred because they reduce the size and cost of key components such as condensers [38, 39]. Additionally, fluids should exhibit favourable liquid-specific heat, viscosity, and thermal stability, which play essential roles in efficient heat transfer and long-term operation. High latent heat and density are also important as they enhance output power and ensure better performance, particularly in combined cycle applications [12, 13]. The molecular weight of the fluid should be compatible with the turbine’s design, and the fluid must be stable under the operational temperatures and pressures, avoiding issues like material degradation or chemical breakdown. Fluids must also be non-corrosive and compatible with turbine materials and lubricating oils to ensure system longevity and minimal maintenance.

Saturation pressure is another important consideration, as higher pressures (typically >100 kPa) are required to prevent air or gas infiltration, which could reduce system efficiency [39]. At the

same time, fluids with moderate heat exchanger pressures are preferred because they allow for safer and more manageable system designs. Overall, the selection of a working fluid that balances these thermodynamic and material compatibility properties is essential for optimizing both performance and cost [40].

Working fluids can be categorized into three main types based on the slope of their temperature-entropy (T-S) saturation curve during the expansion process: wet fluids, dry fluids, and isentropic fluids. Wet fluids, such as water, exhibit a negative slope, which means that during expansion, condensation occurs, leading to two-phase mixtures of liquid and vapour [3]. This can cause erosion in turbines due to the presence of liquid droplets, making wet fluids less desirable for ORC systems. Dry fluids, including hydrocarbon gases such as propane, butane, pentane, and hexane, exhibit a positive slope, meaning that they remain in a superheated vapor state during expansion, avoiding condensation and preventing turbine erosion [41]. Isentropic fluids, such as toluene and R245fa, exhibit a vertical slope and maintain an ideal balance during expansion [1]. However, their high GWP has made them less favourable for use in ORC systems due to environmental concerns.

Historically, water has been widely used as a working fluid in large-scale Rankine cycles, especially in high-temperature, fossil fuel-fired plants. However, at lower temperatures, water becomes less efficient due to its high specific heat and latent heat of vaporization. This makes it unsuitable for ORC applications, which often operate at lower temperatures [42]. Organic fluids, on the other hand, offer significant advantages over water in ORC systems. They require less heat to evaporate and eliminate the need for superheating, making the cycle design simpler and more efficient [43]. These organic fluids generally maintain a superheated vapor state during isentropic expansion through a turbine, preventing the formation of two-phase mixtures and simplifying turbine design [44]. As a result, ORC systems can operate with less complexity, reduced risk of turbine erosion, and lower maintenance costs.

One of the most significant advantages of using dry working fluids in ORC systems is their ability to maintain the superheated vapor state throughout the expansion process [45]. This prevents the formation of liquid droplets that could damage turbine blades, making dry fluids more desirable than wet fluids for ORC applications. Although isentropic fluids offer good thermodynamic properties, their higher global warming potentials (GWP) has led to a decline in their use, especially as global efforts to reduce greenhouse gas emissions intensify. Additionally, organic fluids derived from petroleum exhibit lower evaporation energy than water, requiring less heat for vaporization [46, 47]. This makes them particularly well-suited for ORC systems that operate at lower temperatures, such as those used in geothermal, waste heat recovery, and solar thermal applications [48, 49].

As the need for sustainable and efficient energy solutions grows, the choice of working fluids in ORC systems is increasingly guided by both environmental considerations and performance metrics [50]. The focus is shifting towards fluids that not only offer high efficiency but also align with stricter environmental regulations. In response to these challenges, research and development efforts continue to focus on discovering new working fluids with low GWP, zero ODP, and optimal thermodynamic properties to improve the overall sustainability and performance of ORC systems.

2.2. Material challenges in Geothermal ORC systems

Geothermal Organic Rankine Cycle (ORC) systems operate under extreme conditions due to the high temperature, pressure, and chemically aggressive nature of geothermal fluids. These factors lead to significant material degradation, particularly corrosion in turbines, heat exchangers, and pipelines. The selection of corrosion-resistant materials is crucial to ensuring the long-term durability and efficiency of ORC components. This section explores the major corrosion mechanisms affecting these components and highlights materials that have demonstrated resilience in harsh geothermal environments [51].

Corrosion in geothermal ORC systems arises primarily due to the presence of dissolved gases such as carbon dioxide (CO_2) and hydrogen sulfide (H_2S), as well as chloride-rich geothermal brines. General corrosion occurs when the entire surface of a material undergoes uniform degradation due to its reaction with geothermal fluids, often leading to thinning and structural weakness over time. In contrast, localized corrosion, such as pitting and crevice corrosion, occurs in specific areas where aggressive ions concentrate, leading to rapid penetration and failure of the material [52]. Stress corrosion cracking (SCC) is another prevalent issue in geothermal environments, resulting from the combined effects of tensile stress and corrosive fluid interactions, which can lead to sudden material failure, particularly in turbine blades and piping. Additionally, erosion-corrosion accelerates material degradation due to the mechanical impact of high-velocity geothermal fluids carrying

suspended particulates, leading to severe wear and loss of material integrity [53].

2.2.1. Corrosion-Resistant Materials for Geothermal ORC Systems

The selection of appropriate materials for geothermal ORC systems is essential to combat the detrimental effects of corrosion. Stainless steels such as 316L, Duplex 2205, and Super Duplex 2507 are commonly employed due to their excellent resistance to chloride-induced pitting and stress corrosion cracking. These materials contain high levels of chromium, molybdenum, and nitrogen, which enhance their protective passive film formation, thereby improving their resistance in aggressive geothermal environments [52]. Stress corrosion cracking (SCC) is another prevalent issue in geothermal environments, resulting from the combine. Nickel-based alloys, such as Inconel 625 and Hastelloy C-276, exhibit superior performance in highly acidic and oxidizing conditions, making them suitable for heat exchangers and other critical ORC components. Titanium alloys, particularly Ti-6Al-4V, are widely recognized for their exceptional resistance to corrosion in chloride-rich geothermal brines, preventing structural failures in pipelines and other submerged components [51].

Protective coatings and linings serve as additional barriers against corrosion by preventing direct contact between metal surfaces and aggressive fluids. Epoxy and polymer-based coatings are extensively used in pipelines and heat exchangers, providing a non-permeable barrier against chemical attack [52]. Stress corrosion cracking (SCC) is another prevalent issue in geothermal environments, resulting from the combine. Thermal spray coatings, which include metal-based, ceramic, and composite coatings, are often applied to high-temperature components to improve resistance to oxidation and erosion. Ceramic coatings, in particular, are highly effective in geothermal environments due to their excellent thermal stability and chemical inertness. Additionally, composite materials such as fiber-reinforced polymers (FRP) are gaining popularity due to their lightweight nature and remarkable resistance to chemical degradation [53]. Recent advancements in graphene-based coatings have also demonstrated promising results in enhancing the longevity of ORC components by providing ultra-thin, highly corrosion-resistant protective layers.

The effectiveness of corrosion-resistant materials and coatings has been demonstrated in several geothermal ORC plants worldwide. In Icelandic geothermal plants, extensive use of titanium alloys in heat exchangers has significantly reduced failures caused by chloride-induced corrosion [54]. At the Salton Sea Geothermal Field in the United States, nickel-based alloys have been successfully implemented in turbine components to withstand high concentrations of hydrogen sulfide, thereby enhancing operational longevity. In Japan, geothermal facilities have adopted duplex stainless steels in piping systems to prevent stress corrosion cracking, minimizing the risk of catastrophic failures. Ongoing research continues to focus on developing novel materials, hybrid coatings, and composite structures to further improve the durability and efficiency of geothermal ORC systems. Nanostructured materials and self-healing coatings represent particularly promising innovations, as they can actively repair micro-damages and extend the operational lifespan of components [55].

2.2.2. Protective Coatings for Erosion and Thermal Degradation

Protective coatings play a crucial role in enhancing the durability and performance of geothermal ORC system components. These coatings serve as a barrier against erosion, high-temperature degradation, and chemical attack from geothermal fluids. The selection of appropriate coatings depends on factors such as operating temperature, fluid composition, and mechanical stresses encountered in the system [54].

Thermal spray coatings, which include metallic, ceramic, and cermet-based solutions, provide high resistance to oxidation and wear in elevated-temperature environments. Metallic coatings, such as those based on nickel-chromium (NiCr) and molybdenum, form a protective oxide layer that minimizes the effects of high-temperature corrosion [56]. Ceramic-based coatings, including aluminum oxide (Al_2O_3) and zirconium oxide (ZrO_2), offer superior thermal insulation and resistance to chemical attack, making them ideal for use in turbine components and high-temperature heat exchangers. Cermet coatings, composed of tungsten carbide-cobalt (WC-Co) and chromium carbide-nickel-chromium (Cr_3C_2-NiCr), provide exceptional wear resistance, ensuring prolonged durability in harsh geothermal conditions [55].

Polymer-based coatings, including epoxy and polyurethane coatings, are widely used for corrosion protection in geothermal pipelines and heat exchangers. These coatings form an impermeable barrier that prevents direct exposure to aggressive geothermal fluids, thereby mitigating material degradation. Additionally, polytetrafluoroethylene (PTFE) and fluoropolymer coatings offer low surface energy, reducing scaling and biofouling in ORC systems. Recent advancements in nanostructured coatings, such as

graphene and carbon-based solutions, have demonstrated remarkable chemical resistance and mechanical strength, making them attractive candidates for next-generation geothermal applications [56]. The development of self-healing coatings further enhances the reliability of ORC components by enabling autonomous repair of minor damages, thereby extending operational life and reducing maintenance costs [55].

2.2.3. Material Compatibility with Working and Geothermal Fluids

Material compatibility is a critical consideration in geothermal ORC systems to ensure that components can withstand the chemical and thermal conditions imposed by both working fluids and geothermal brines. High-salinity brines pose a significant challenge due to their aggressive nature, necessitating the use of corrosion-resistant materials such as titanium alloys and duplex stainless steels [57]. These materials exhibit exceptional resistance to chloride-induced corrosion, thereby preventing premature failure in pipelines and heat exchangers. Exposure to hydrogen sulfide (H_2S) can accelerate material degradation, particularly in carbon steels. Nickel-based alloys, such as Hastelloy C-276, have proven effective in mitigating sulfide-induced corrosion, ensuring long-term reliability in geothermal environments [58].

Working fluids used in ORC systems also impact material compatibility. Hydrocarbon-based ORC fluids, including isopentane and toluene, require elastomers and seals that resist swelling and degradation. Ammonia-water mixtures, commonly used in Kalina cycle systems, are highly corrosive to copper-based alloys, necessitating alternative material selections. Supercritical CO_2-based ORC systems impose additional challenges, as carbon steel components may experience accelerated degradation under high-pressure conditions. Stainless steels and ceramic coatings have demonstrated improved resistance in such environments, offering viable solutions for long-term durability [57].

2.3 Material Behavior under Geothermal Conditions

2.3.1. Impact of Geothermal Fluids on Material Degradation

The study of material degradation in geothermal Organic Rankine Cycle (ORC) systems requires a thorough investigation of the effects of geothermal fluids on structural materials over extended periods. Laboratory and field studies have been conducted to analyze corrosion, scaling, and material deterioration under geothermal conditions. These studies provide critical insights into how different material compositions perform in aggressive environments characterized by high salinity, dissolved gases, and elevated temperatures [59].

Electrochemical and accelerated aging tests serve as fundamental methods for evaluating corrosion rates and predicting material longevity. Electrochemical impedance spectroscopy (EIS) and potentiodynamic polarization techniques are widely used to assess the passivation behavior of metals and alloys in geothermal brines. Accelerated aging tests, including high-temperature autoclave exposure and cyclic immersion tests, replicate the long-term effects of geothermal fluids on materials within a controlled timeframe [60]. By systematically studying the degradation behavior of materials such as carbon steel, stainless steel, nickel-based alloys, and titanium alloys, researchers can determine their suitability for geothermal ORC applications.

Comparative studies between conventional and advanced materials reveal significant differences in their resistance to geothermal-induced degradation. While carbon steels remain susceptible to pitting and stress corrosion cracking in chloride-rich environments, duplex stainless steels and superalloys demonstrate superior resistance, attributed to their enhanced passive film stability and alloying elements such as chromium and molybdenum [60]. Titanium-based materials exhibit exceptional corrosion resistance but pose economic constraints due to their high cost. The incorporation of protective coatings further enhances material performance by providing an additional barrier against aggressive geothermal fluids [61].

2.3.2. Performance of Advanced Materials and Coatings

The effectiveness of corrosion-resistant alloys and coatings in geothermal ORC systems has been extensively investigated through experimental testing and numerical simulations. Numerous studies have examined the application of thermal spray coatings, polymer-based linings, and advanced ceramic coatings in mitigating wear, corrosion, and high-temperature degradation. Experimental methods, such as scanning electron microscopy (SEM) and X-ray diffraction (XRD), provide in-depth characterization of coating integrity and failure mechanisms under extreme conditions. These techniques help assess the adhesion strength, porosity, and microstructural evolution of coatings subjected to geothermal environments [62].

Computational methods play an increasingly vital role in predicting material behavior under

geothermal conditions. Computational fluid dynamics (CFD) and finite element analysis (FEA) are widely employed to simulate fluid-material interactions and predict the effects of erosion, scaling, and thermal stress on ORC components. CFD modeling enables the evaluation of fluid velocity profiles and turbulence-induced degradation, allowing engineers to optimize pipeline and heat exchanger designs for reduced wear [63]. FEA simulations assess mechanical stresses imposed on materials due to cyclic thermal loading and pressure fluctuations, ensuring that critical components such as turbine blades and heat exchanger tubes maintain structural integrity over prolonged operational periods.

In addition to experimental and computational studies, ongoing research is dedicated to identifying novel materials that offer enhanced durability in geothermal ORC applications. Graphene-based coatings, self-healing polymers, and nano-structured surface modifications are among the emerging technologies being explored for their ability to resist corrosion and erosion while maintaining mechanical strength [63]. These advanced materials promise to extend component lifespan and reduce maintenance requirements, thereby improving the economic feasibility of geothermal ORC plants [64].

2.3.3. Strategies for Enhancing ORC Component Lifespan

Ensuring the longevity of ORC system components requires the implementation of effective maintenance, monitoring, and material selection strategies. The use of corrosion inhibitors, for example, has proven beneficial in reducing the rate of material degradation by forming protective films on metal surfaces. Chemical treatments involving phosphate- and molybdate-based inhibitors have demonstrated success in geothermal applications by minimizing localized corrosion in heat exchangers and pipelines [65].

Predictive maintenance, enabled by real-time monitoring technologies, provides a proactive approach to identifying material degradation before catastrophic failures occur (Izuwa et al., 2024). Sensors equipped with electrochemical monitoring capabilities can detect changes in material passivation and corrosion rates, allowing operators to take preventive action. Non-destructive testing (NDT) methods, such as ultrasonic thickness gauging and eddy current testing, further contribute to the early detection of material wear and structural defects, facilitating timely repairs and replacements [64].

Material innovations, including self-healing coatings and nano-structured materials, offer promising advancements in extending the service life of ORC components. Self-healing coatings, which contain microencapsulated corrosion inhibitors, can autonomously repair minor surface damages, preventing the initiation of corrosion sites. Nanostructured surface treatments, such as plasma-assisted deposition techniques, enhance material resistance to erosion and fouling by altering surface roughness and chemical reactivity [66].

Best practices in material selection remain paramount to optimizing ORC system durability. The integration of duplex stainless steels, nickel-based superalloys, and advanced ceramic coatings ensures that components can withstand the combined effects of geothermal fluid exposure and thermal cycling [67]. By aligning material selection with the specific operating conditions of geothermal ORC systems, engineers can minimize unplanned downtime, reduce maintenance costs, and enhance overall system efficiency [68]. Continuous research and technological advancements in material science will further contribute to the development of next-generation materials capable of withstanding the extreme conditions of geothermal ORC environments, thereby ensuring sustainable and long-term energy production [69].

3. METHODS

The method consists of three different parts including the process simulation of the geothermal binary ORC system for electricity generation, the implementation of the surrogate models comprising RSM and ANN to investigate the interrelationship between influencing parameters and output, and the model optimisation using RSM and ANN-GA for optimal parameter conditions. The methods comprise the following

- Process modelling using Hysys to conduct modelling and simulation of geothermal binary ORC system using water and isopentane as geofluid and working fluid respectively and in conducting simulation runs for different input datasets generated with the Box-Behnken design (BBD) method
- Developing surrogate model for RSMmodelling and ANN modelling using Design Experts and MATLAB respectively to determine the relationship between decision variables and output response and approximate the design space.
- Perform optimization based on the modelled design space using RSM optimization and a coupled artificial neural network model and genetic algorithm (ANN-GA)

3.1. Process Modelling and Simulation

3.1.1. Process Model

The model utilised by Hysys is based on mass and energy balance in steady state condition. The

steady-state energy models for the ORC system are given below

$$\sum \dot{m}_{in} = \sum \dot{m}_{out} \quad (1)$$

$$\sum Q + \sum \dot{m}_{in} h_{in} = \sum W + \sum \dot{m}_{out} h_{out} \quad (2)$$

$$W_{net} = W_{turbine} - W_{pump} \quad (3)$$

$$W_{turbine} = \dot{m}_f (h_{in} - h_{out}) \quad (4)$$

Where $\dot{m}$ (kg /s) is the mass flow rate, h is the specific enthalpy of the system's working fluid streams, (kJ/kg), Q represent the heat energy passing via the component boundaries, (Watts), W is the work energy passing via the component boundaries, (Watts), Wnet is the net work, Watts, Wturbine is the turbine work, Watts, Wpump is the pump work, Watts, $\dot{m}_f$ is the mass flow rate, hin is the specific enthalpy at the turbine entry, hout is the specific enthalpy at the exit of the turbine

3.1.2. Model Simulation

The simulation model made with Aspen Hysys v11 software consists of; Evaporator, Turbine, Condenser, and Circulating Pump. The model consists of three different loops; first the heating loop which is the hot water rising from the abandoned oil and gas well, the ORC loop which is the working fluid (i-C_2H_5), and finally the cooling cycle for the condenser which is also water.

The scheme of the ORC power plant is shown in Fig. 1, displaying the heating loop which is the hot water rising from the abandoned oil and gas well, the ORC loop which is the working fluid (i-C_2H_5), and finally the cooling cycle for the condenser which is also water. An ORC power cycle utilizing i-C_2H_5 as working fluid is fed (stream #3) through a condensing heat exchanger (E100 and E101), which is pressurized at about 10 bars. The ORC scheme comprehends an evaporator, a turbine, a condenser, and a pump which were modelled as heat exchangers, expander, air cooler and pump in Hysys respectively. The process flow diagram (PFD) for the ORC process simulated in Hysys is given in Figure 3

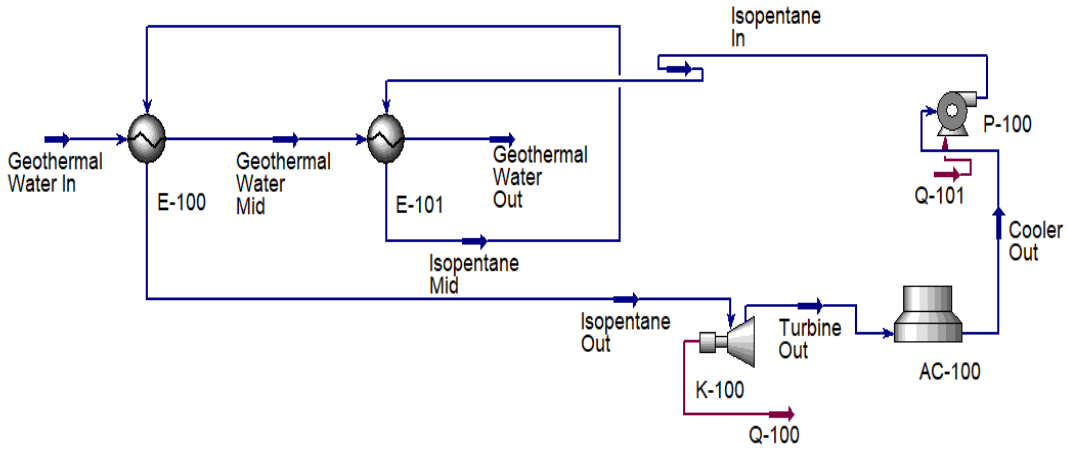

Figure 1. Process flow diagram (PFD) of the geothermal binary ORC system

The geofluid which is hot water comes from the wells and enters into HEX1 (E-100) and subsequently to HEX2 (E-101). iC_2H_5 is pumped into the heat exchangers and extracted heat both from HEX2 and HEX1 and then exits HEX1 towards the turbine. At the turbine, iC_2H_5 was vapourised andexpandedthus rotating the turbine leading to the generation electric power. The iC_2H_5 exits the turbine at lower temperature and pressure and goes to the air cooler where it is cooled and then pumped back to the HEXs to continue the cycle. Water that came out from the outlet of HEX2 was injected back into the well and the cycle continues. Throughout the process, the turbine, pump, and compressor stages are assumed to be adiabatic devices. Negligible pressure losses occur in the components of the ORC and its piping system. Neglecting the changes of kinetic and potential energies, the mass and energy balance equations in the steady-state condition can be applied to each component.

3.2. Development of Surrogate Model

The surrogate model comprises the RSM and ANN conducted to investigate the relationship between input parameters and power produced. The surrogate models are applied to dual functions which includes design space approximation and optimisation.

3.2.1.RSMModelling

A response surface methodology (RSM) model was implemented using Design-Expert software to predict geothermal power generation by applying regression analysis to the experimental data obtained through a Box-Behnken design (BBD). The BBD incorporated three independent variables which were found to have impact on the geothermal power generation; these include:

working fluid (iC2H5) flowrate (kg/s), working fluid inlet pressure (bar) and turbine outlet pressure (bar). Several regression models were tested and evaluated to identify the one with the highest performance and accuracy, most the independent variables. The flowchart in Figure 2 illustrates the steps involved in the RSM modelling. The RSM selected the best regression model based on statistical parameters such as R^2, adjusted R^2, predicted R^2, standard deviation, and coefficient of variation (COV). Multiple regression analyses facilitated the fitting of these models to the simulation data, allowing for the estimation of responses from independent variables using their general equations. Some of the equations for several models in RSM is given below.

The general form of the models for linear regression is given as

$$y = a_o + \sum_{i=1}^{k} a_i x_i + e \quad (5)$$

The general form of the 2FI regression model is given as

$$y = a_o + \sum_{i=1}^{k} a_i x_i + \sum_{i<j}^{k} a_{ij} x_i x_j + e \quad (6)$$

The general form of the quadratic regression model is given as

$$y = a_o + \sum_{i=1}^{k} a_i x_i + \sum_{i<j}^{k} a_{ij} x_i x_j + \sum_{i=1}^{k} a_{ii} x_i^2 + e \quad (7)$$

Where x_i,x_j, x_l, are the input variables and a_i, a_{ij}, a_{ii},and a_{ijl} are the coefficient of each of the terms, a_o is the offset and e is the residual or error term

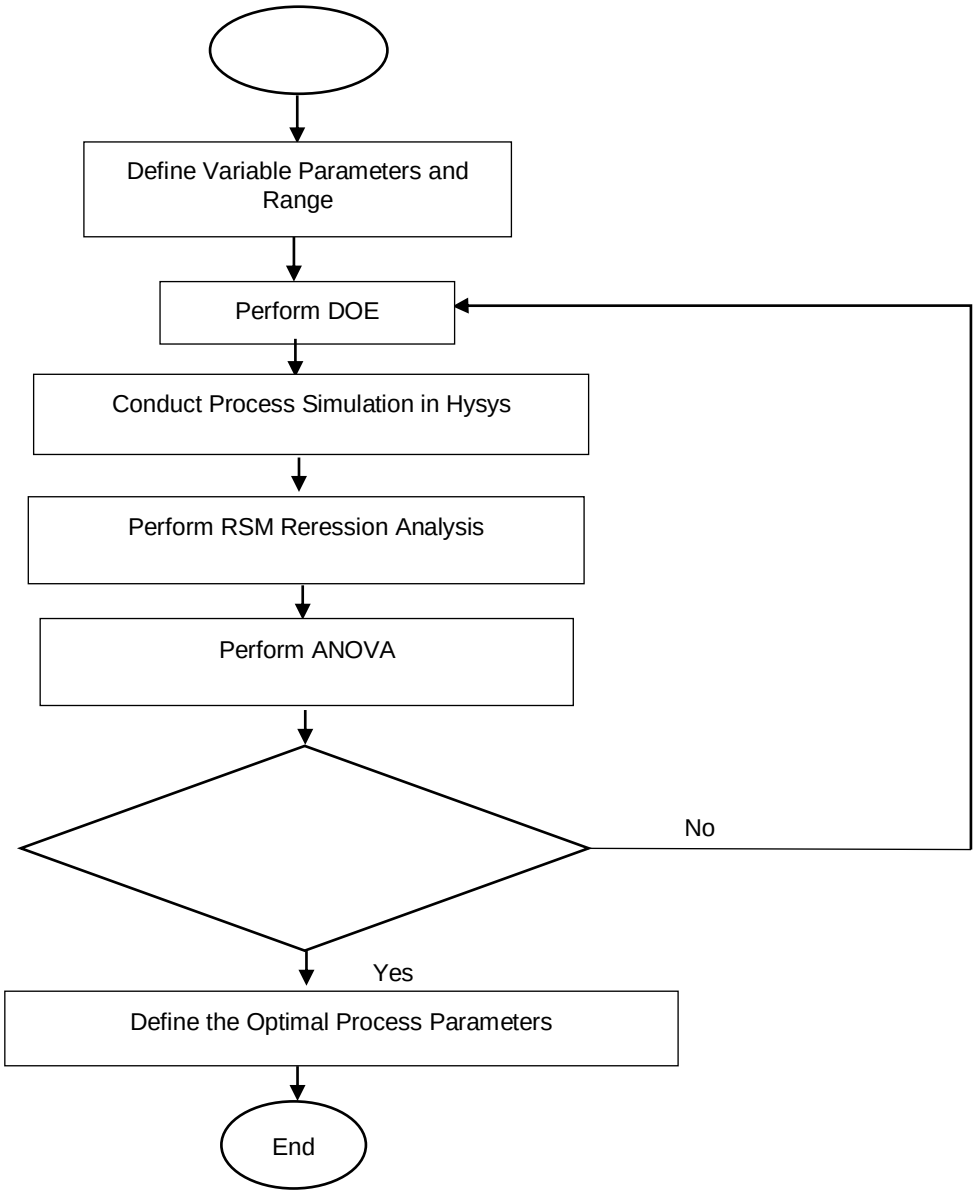

Figure 2. RSM Modelling Flowchart

3.5.2. ANN Modelling

The ANN model was developed using MATLAB by training with simulation data from the BBD, aiming to create a network capable of accurately modellinggeothermal power generation based on the input of independent variables. The model was constructed using a dataset of 17data points, with 70% of the data allocated for training, 15% for testing, and 15% for validation. The ANN model employed in this study utilizes a feed-forward neural network architecture, following the backpropagation learning principle. The network architecture consists of an input layer, a hidden layer, and an output layer. Various configurations of neurons in the hidden layer were tested, with the optimal network topology determined iteratively by evaluating network performance indices. Training of the network was performed using the Levenberg-Marquardt (LM) algorithm, with the Sigmoid function used as the transfer function. The optimal number of neurons in the hidden layer was selected based on the best performance, measured by the R^2 value and root mean squared error (RMSE).

The construction of an ANN model involves adjusting weights and biases. The output of a neuron is computed by summing the weighted inputs and adding a bias, which is then processed through a transfer function.

$$f_n = f\left[\left(\sum_{i=1}^{k} w_i\, x_i\right) + b\right] \qquad (8)$$

Where k, wi, b, and f(n) are the number of elements in the input vector xi, the interconnection weight, the bias for the neuron (n), and the neuron output, respectively. ANNs feature various network architectures, training algorithms, transfer functions, and optimal neuron counts [70]. The ANN model employed in this study utilizes a feed-forward neural network architecture based on the backpropagation learning principle. For training nonlinear functions, such as those encountered in many chemical processes, the tangent sigmoid transfer function (tansig) is commonly used due to its effectiveness. The general formula for the tansig transfer function is given as follows:

$$f(x) = \frac{2}{1 + e^{-2x}} - 1$$

Additionally, following the recommendations of Hojjat et al. [71], input parameters were normalized by dividing each column by its maximum value, ensuring a range of zero to one (0–1). The study utilized these normalized parameters as inputs for modelling the artificial neural network.

The structure of the network is illustrated in Figure 3.

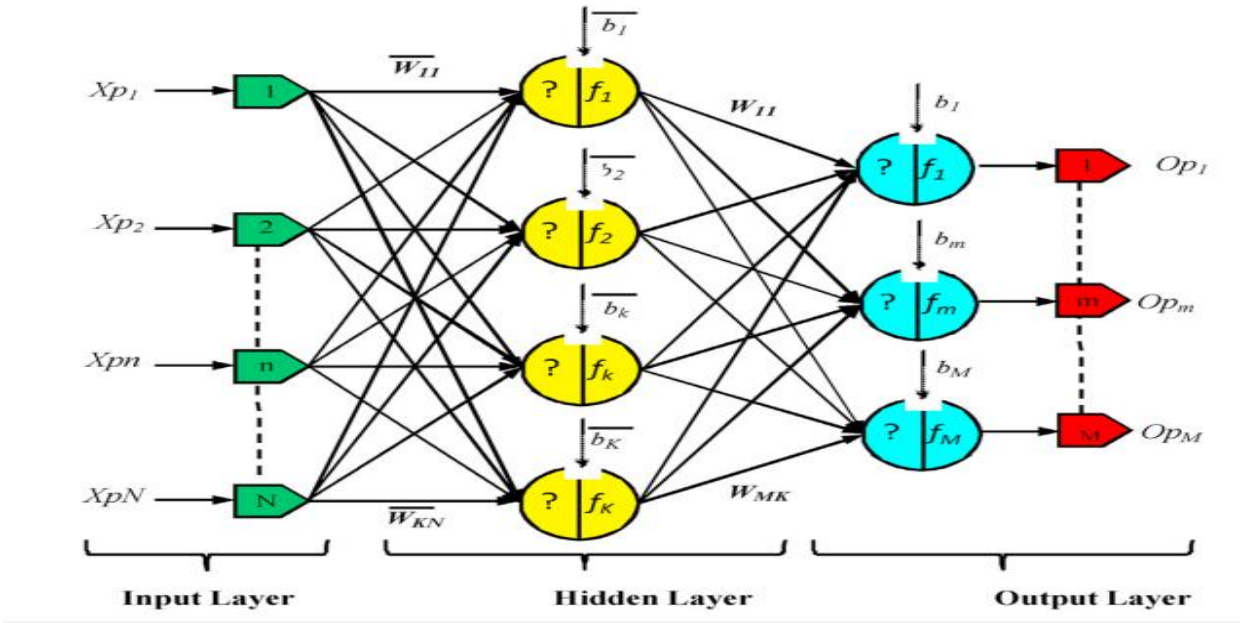

Figure 3. Sample network architecture for ANN modeling [27]

The flowchart in figure 3 describes the steps of the ANN modelling

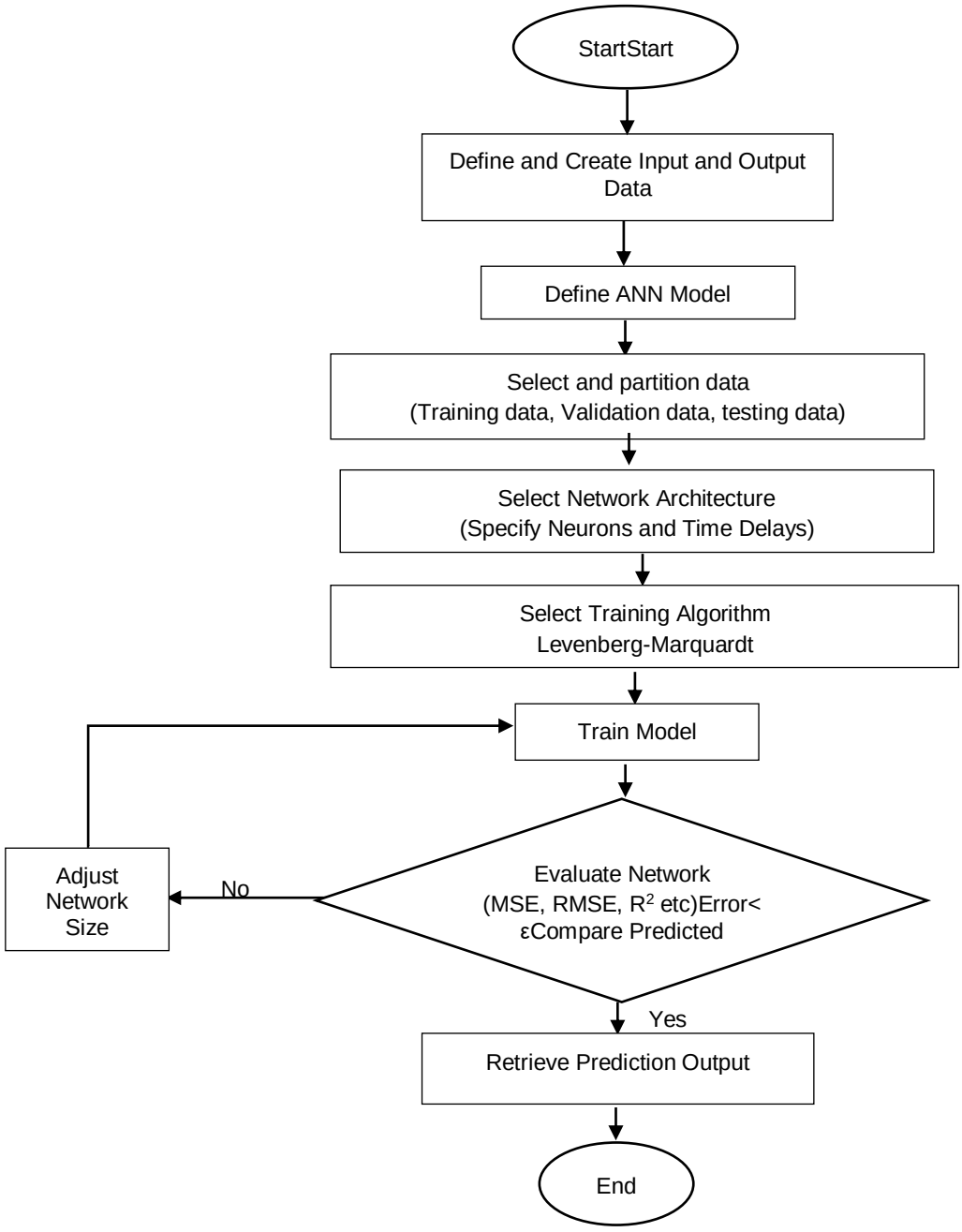

Figure 4. ANN Modelling Flowchart

3.2.3. Performance Metrics of Surrogate Models

The predicted power generation from RSM and ANN models were assessed and compared in terms of statistical performance metricsincluding coefficient of determination (R^2), adjusted, standard deviation and root mean squared error (RMSE). The formulas for these metrics are given:

$$R^2 = \frac{\sum_{i=1}^{n}\left(x_{a,i}-x_{p,i}\right)^2}{\sum_{i=1}^{n}\left(x_{p,i}-x_{a,ave}\right)^2} \quad (11)$$

$$AdjustedR^2 = 1-\left[(1-R^2)\times\frac{n-1}{n-k-1}\right] \quad (12)$$

$$RMSE = \sqrt{\frac{1}{n}\sum_{i=1}^{n}\left(x_{p,i}-x_{a,i}\right)^2} \quad (13)$$

Where n is the number of experimental runs $x_{p,i}$is the estimated values, $x_{a,i}$is the experimental values, $x_{a,ave}$ is the average experimental values, k is the number of input variables

3.6.4. Power Generation Optimization

Optimization was carried out using both Response Surface Methodology (RSM) and artificial neural network coupled Genetic Algorithm (ANN-GA). Initially, a quadratic model was

developed through RSM. This model was optimized using RSM itself, and then it was exported to MATLAB, where GA was applied for further optimization. This process yielded two distinct optimization outcomes—one from RSM and the other from GA. These results were subsequently compared, focusing on the values of the independent variables and the resulting optimized power generated.

4. RESULTS

The results for power generationfrom the surrogate models conducted is presented in this section which model result results from RSM and ANN, and optimisation results from RSM and ANN-GA.

4.1. Results for RSM analyses

The results of the RSM modelling are presented and discussed in this section, encompassing Table 1, Table 2, and Table 3. These tables display both the actual output from the process simulation and the corresponding predicted output responses from RSM, considering input variables such as working fluid flowrate, working fluid outlet pressure and turbine outlet pressure. Among several regression models tested, the quadratic model demonstrated the highest fit to the actual data for as shown in Table 1 and was selected for its superior prediction accuracy. Equation 20 is the quadratic model generated by RSM for the power generation.

Table 1. Error data for RSM model analyses

Source	P value	R^2	Adjusted R^2	
Linear	<0.0001	0.8850	0.8145	
2FI	0.1381	0.9117	0.7587	
Quadratic	0.0001	0.9923	0.9462	Suggested
Cubic		1.0000		Aliased

$$\textit{Power Generation (kWh)} = 475.8 + 144.374\,A + 243.491B - 76.9425C + $$

$$+ 81.0775AB - 26.025AC + -3.99BC + 0.15625A^2 - 96.3788B^2 + 11.2188C^2$$

Where variables A, B, C represent working fluid flowrate (kg/s), working fluid inlet pressure (bar) and turbine outlet pressure (bar) respectively.This equation can be utilized to predict the response for given levels of each factor. To achieve accurate predictions, the levels must be specified in the original units of each factor, both for the input parameters and the response variables. To assess the significance of the model coefficients, Analysis of Variance (ANOVA) was conducted. Table 2 and Table 3 summarize the ANOVA results and fit metrics for the power generation output responses. These tables include degrees of freedom, mean square values, F-values, and p-values. In Table 5, the p-values are smaller than 0.0001, and the high F-values indicate that the models are statistically significant.

The RSM model's predictions closely matched the actual simulation data, as shown in Table 8. To evaluate the statistical significance of the model, an Analysis of Variance (ANOVA) was conducted on equation 14, as detailed in Table 2. The results indicated that the model was statistically significant ($p < 0.0007$), with a non-significant lack of fit. The adjusted R^2 value (0.9923) and predicted R^2 value (0.9462) further confirmed the model's robustness, suggesting that the key factors influencing power generated—such as working fluid flowrate (kg/s), working fluid inlet pressure (bar) and turbine outlet pressure (bar)—were effectively captured by the model.

Table 2. ANOVA

Source	Sum of Squares	df	Mean Square	F-value	p-value	
Model	7.57E+05	9	84093.51	230.56	< 0.0001	significant
A-Working Fluid Flowrate	1.67E+05	1	1.67E+05	457.19	< 0.0001	
B-Working Fluid Outlet Pressure	4.74E+05	1	4.74E+05	1300.42	< 0.0001	
C-Turbine Outlet Pressure	47361.19	1	47361.19	129.85	< 0.0001	
AB	26294.24	1	26294.24	72.09	< 0.0001	
AC	2709.2	1	2709.2	7.43	0.0295	
BC	63.68	1	63.68	0.1746	0.6886	
A^2	0.1028	1	0.1028	0.0003	0.9871	
B^2	39111	1	39111	107.23	< 0.0001	
C^2	529.94	1	529.94	1.45	0.2672	
Residual	2553.12	7	364.73			
Lack of Fit	2553.12	3	851.04			
Pure Error	0	4	0			
Cor Total	7.59E+05	16				

Figure 5 shows the relationship between the actual and predicted results from the RSM model

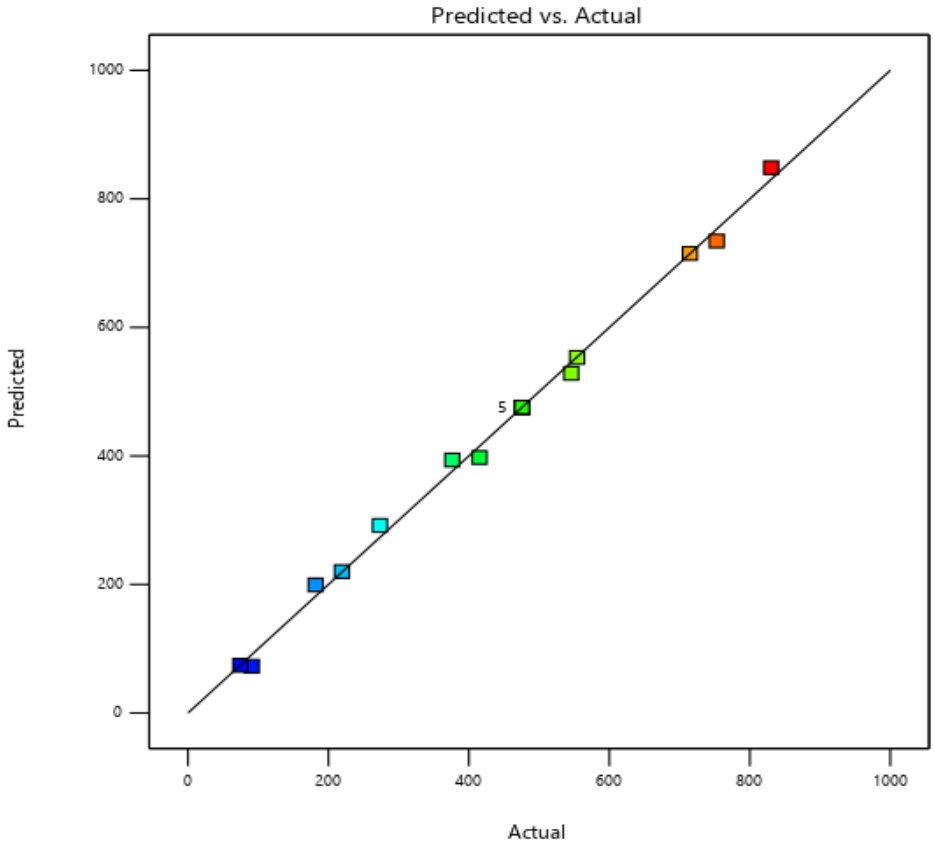

Figure 5.Parity plot of Actual vs Predicted values of power generated from RSM model

The parity plot in figure 4 shows how the data points from the actual (process simulation datal) and predicted power generated clustered aroun the 45^{o} line. This figure demonstrate that the actual and predicted output responses closely align around the 45-degree line for all indicating strong regression and agreement between the two datasets. Thus, there exists an acceptable level of agreement between the actual process simulation data and the predicted responses from the RSM models.

4.2. Interaction Response of Input Parameters on Power Generated using 3D Plots

Figure 6 illustrates the 3D response surface plot depicting the interaction between independent variables and power production while figure 7 shows the contour plots for the power production from the RSM modelling. These plots visually represent how changes in the independent variables (such working fluid flowrate (kg/s), working fluid inlet pressure (bar) and turbine outlet pressure (bar)) influence the power production providing insights into their mutual interactions.

Both the 3D surface plots in figure 6a-c and the contour plots in Figure 7a-c are used to make analysis of the interactions between the independent variables and the response.

Figure 6a and Figure 7a shows the interactive effect of working fluid flowrate and working fluid outlet pressure on the power generated. As can be observed, increasing the working fluid flowrate increases the power generated by the binary ORC system at higher outlet pressures of the working fluid. In other words both the flowrate and outlet pressures of the working fluid have positive effect on the power generated as their increase results to higher power generated.

Figure 6b and Figure 7b shows the interactive effect of working fluid flowrate and turbine outlet pressure on the power generated. It can be observed that at lower turbine outlet pressures, increasing the flowrate of the working fluid increases the power generated by the turbine. However, when the flowrate of the working fluid is kept constant, the power generated by the turbine decreases as the turbine outlet pressure increases.

Figure 6c and Figure 7c shows the interactive effect of working fluid outlet pressure and turbine outlet pressure on the power generated. It is seen that at lower turbine outlet pressures, increasing

the outlet pressure of the working fluid increases the power generated by the turbine. However, when the outlet pressure of the working fluid is kept constant, the power generated by the turbine decreases as the turbine outlet pressure increases.

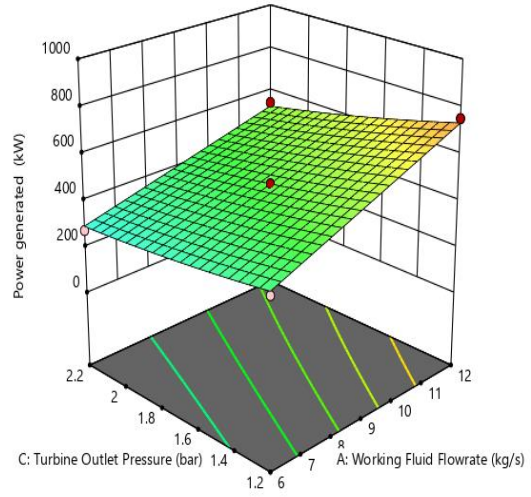

a)

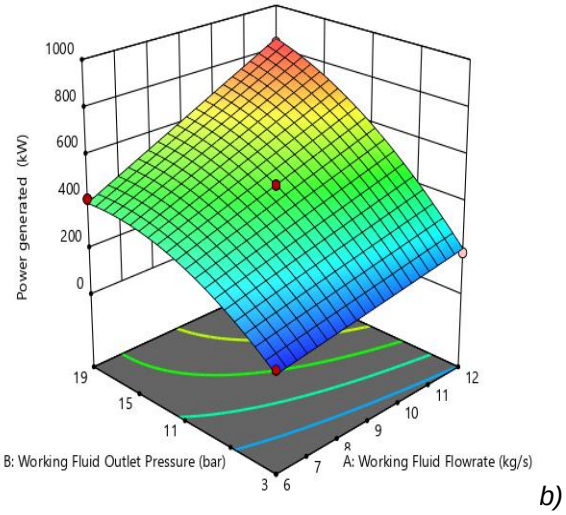

b)

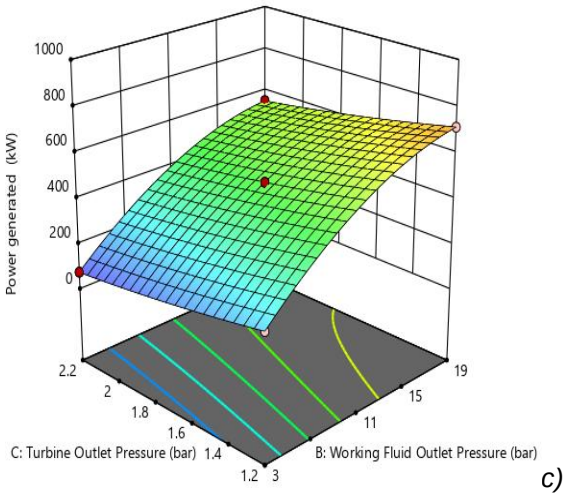

c)

Figure 6. 3D response surface plots for power production from RSM

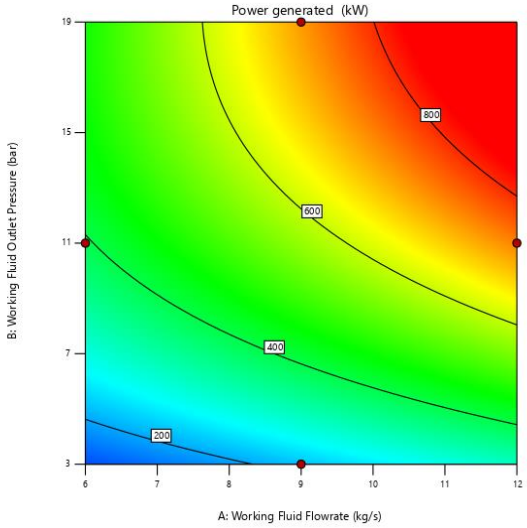

a)

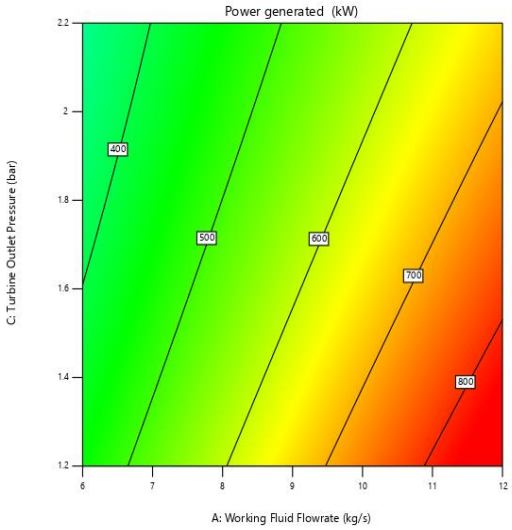

b)

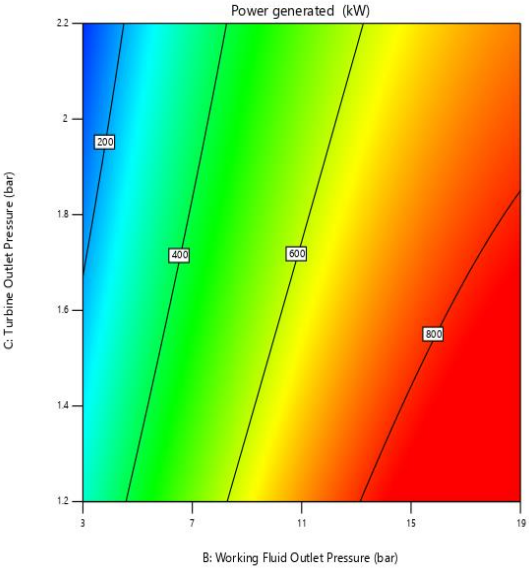

c)

Figure 7. Contour plots for power production from RSM

4.3. Results for ANN Modelling

The ANN neural network model was employed to establish the relationship between the input factors and the output response. The selection of the optimal neural network for the ANN analysis was based on the performance of various transfer functions, training algorithms, network architectures, and the optimal number of neurons. Multiple training sessions were conducted, and the best-performing results were selected to represent the model. The performance of these factors was evaluated using metrics such as R^2 values, mean squared error (MSE), root mean squared error (RMSE), mean absolute error (MAE), and mean absolute percentage error (MAPE). A higher R^2 value, along with lower MSE, RMSE, MAE, and MAPE values, indicates better predictive accuracy in relation to the model's factors. The R-value corresponding to the selected trained ANN model is presented in Figure 6.

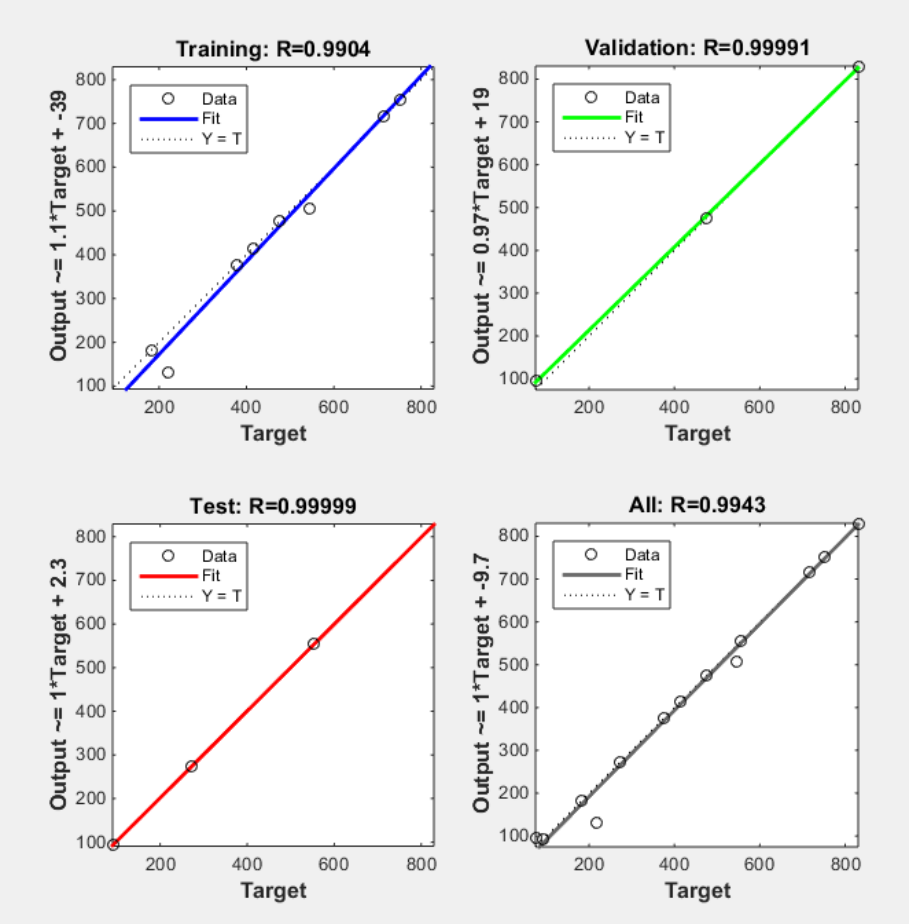

Figure 8.Regressionplot for the training in ANN

Figure 8 shows the Regression values corresponding to the ANN training performed. The Overall R values for the ANN model was 0.9943. It is seen that ANN gave notably high R values which indicate very good predictions for the power generated.

Table 4 shows the values predicted by RSM and ANN models for each of the input variables and actual output data. Table 4 shows that there is a high correlation between the actual and predicted results for the RSM and the ANN models.

Table 4. Actual and predicted results for power generated corresponding to RSM and ANN modelling.

Run	Working Fluid Flowrate, kg/s	Working Fluid Outlet Pressure bar	Turbine Outlet Pressure, bar	Actual Power Generated kW	RSM Predicted Power Generated, kW	ANN Predicted Power Generated, kW
1	9	11	1.7	475.8	475.8	475.9489
2	6	19	1.7	415.2	397.62	415.1577

3	9	11	1.7	475.8	475.8	475.9489
4	12	11	1.2	753	734.52	753.0379
5	9	19	1.2	714.7	715.06	714.7729
6	12	3	1.7	181.8	199.38	181.8843
7	6	11	1.2	376.5	393.72	376.4783
8	9	11	1.7	475.8	475.8	475.9489
9	9	3	2.2	74.56	74.2	94.31542
10	9	11	1.7	475.8	475.8	475.9489
11	6	3	1.7	90.91	72.79	93.33428
12	6	11	2.2	273.4	291.88	273.4133
13	9	19	2.2	554.1	553.2	554.146
14	9	11	1.7	475.8	475.8	475.9489
15	12	11	2.2	545.8	528.58	505.9555
16	9	3	1.2	219.2	220.1	132.1279
17	12	19	1.7	830.4	848.52	829.374

Table 5 shows the comparison of performance metrics for the RSM and the ANN predictions.

Table 5: Performance metrics for RSM and ANN Predictions

	RSM	ANN
MSE	150.1611	562.7336
RMSE	12.2540	23.7220
MAE	8.5482	8.8932
MAPE	0.0318	0.0450
R^2	0.9966	0.9886

From Table 5, it is seen that both RSM and ANN models gave realistic predictions of the actual/experimental data for the error metrics considered. In terms of R^2 values, both RSM and ANN gave predictions higher than 0.9 which indicates very good predictions of the test data. The R^2 values for RSM was 0.9966, while that for ANN was 0.9886. Thus, relative to R^2 values the RSM performed better than the ANN. The MSE and MAE of RSM model were 150.1611 and 12.2540 respectively while the MSE and MAE for ANN were 562.7336 and 23.722respectively. The MAPE of RSM and ANN models were 3.18% and 4.5% respectively it is evident that the RSM performed better than the ANN model.

Additionally, the model performance in this study were compared with performance of scholars who conducted modelling on geothermal systems as summarized in Table 6.

Table 6. Comparison of model performance of study with results from literature

Area of Study	Target Parameter	Model Used	R2	RMSE	Reference
Binary Geothermal Power Plant	Power Generated	ANN	0.999	0.272	[27]
Double Flash Cycle Geothermal Turbine to	Net Power Generated	Multiple Linear Regression	-	0.9997	[72]
Geothermal Binary ORC Systems	System Performance	Taguchi model	0.941	4.29	[73]
Geothermal ORC system	Power Generated	ANN	0.9986	51.2	[74]
Geothermal ORC system	Turbine performance	ANN	0.9989	0.0009	[25]
Enhanced Geothermal systems	Geothermal production temperature	ANN	0.998	0.067	[75]
Geothermal Binary ORC system	Power Generated	ANN	0.9886	23.7220	This Study
		RSM	0.9966	12.2540	

Table 6 shows the performance of various studies on geothermal systems using various modelling techniques in describing the relationship between the input parameters and the target output. It can be observed that from literature several models have been successfully utilised for modelling geothermal systems with excellent performance. Moreso, it is seen that the performance of the ANN and RSM model realised in this study are close to the performances seen in literature in several studies conducted on geothermal systems especially in the area of

geothermal binary ORC systems for power generation.

4.4.Optimisation of Power Generated

Table 7 gives the summary of the optimisation results of power generated corresponding to RSM and ANN-GA optimisations performed.

Table 7. Optimisation results

Parameter	RSM	ANN-GA	Hysys Check
Working fluid flowrate, MMscfd	11.8	12	12
Working fluid outlet pressure, bar	18.47	19	19
Turbine outlet pressure	1.2	1.2	1.2
Power generated, kW	940.78	958.48	952.9
Power Generated from Hysys at optimal factors, kW	927.2	952.9	-
Percentage error	1.46	0.59	-

Table 7 provides a comparative analysis of the optimization results obtained using two distinct methodologies: Response Surface Methodology (RSM) and the coupled Artificial Neural Network-Genetic Algorithm (ANN-GA). These optimization techniques adopt fundamentally different approaches, which naturally result in variations in their outcomes. To evaluate their performance, an optimization check was conducted in Aspen HYSYS to determine the optimal input factors based on sensitivity analysis trends. The optimal input variables predicted by both methods were subsequently inputted into HYSYS to verify the corresponding power output.

From the results presented in the table, it is evident that ANN-GA demonstrated superior optimization capabilities. The method accurately predicted the ranges of input variables—working fluid flowrate, working fluid outlet pressure, and turbine outlet pressure—that yielded the optimal power output. The optimal values identified by ANN-GA were consistent with those determined directly by HYSYS, signifying excellent alignment and optimization performance. This consistency highlights the robustness and reliability of ANN-GA in predicting the key input parameters required for maximizing power generation.

In contrast, RSM struggled to accurately predict the optimal input values. Although RSM provided a set of predicted optimal factors, these values deviated from the actual optimal values determined by HYSYS. To further assess the optimization performance of both methodologies, their predicted input values were tested in HYSYS, and the corresponding power outputs were analyzed. ANN-GA achieved a power output of 958.48 kW when its predicted values were inputted, closely matching the 952.9 kW output determined directly by HYSYS. This resulted in a percentage error of just 0.59%, demonstrating the high accuracy of ANN-GA not only in parameter prediction but also in achieving optimal power generation.

On the other hand, the power output generated using the input factors predicted by RSM was 927.2 kW when tested in HYSYS. This value significantly deviated from the 940.78 kW predicted by RSM itself, resulting in a higher percentage error of 1.46%. The discrepancy between RSM's predicted and actual performance highlights its limitations in identifying the precise input variables required for maximum power generation. Moreover, the power output achieved by RSM was considerably lower than the optimal power output obtained via ANN-GA, further emphasizing the comparative weakness of RSM as an optimization tool for this process.

The analysis highlights the robustness and accuracy of the ANN-GA model, which not only closely aligned with HYSYS predictions but also consistently delivered power outputs that were nearly identical to the actual optimal values. Its integration of machine learning (via ANN) and evolutionary optimization (via GA) likely contributed to its superior performance by effectively capturing complex nonlinear relationships and exploring the solution space more comprehensively. ANN-GA significantly outperformed RSM in optimization performance. While RSM exhibited notable errors and limitations, ANN-GA proved to be a highly reliable and robust optimization technique, demonstrating its potential as a powerful tool for process optimization in scenarios where accuracy and efficiency are paramount.

5. CONCLUSION

Modelling and optimization of geothermal binary Organic Rankine Cycle (ORC) systems has been accomplished in this study, leveraging Aspen HYSYS process simulations with RSM and ANN models. Aspen HYSYS was utilized to model the process system and generate simulation data, which served as the foundation for developing RSM and ANN models. The RSM and ANN models were designed using the Box-Behnken Design (BBD) for three factors: working fluid flowrate, working fluid outlet pressure, and turbine outlet pressure, while optimization was performed independently using RSM and ANN-GA.

In terms of modelling, both RSM and ANN demonstrated excellent capabilities in capturing the nonlinear relationships between the input parameters and the system's power generation. The RSM model, however, outperformed ANN with a superior coefficient of determination (R^2) of

0.9966 compared to 0.9886 for ANN. Additionally, the RSM model achieved a lower root mean square error (RMSE) of 12.254 compared to ANN's RMSE of 23.722, highlighting its superior predictive accuracy and robustness in modeling the system's behavior.

When applied to optimization, the ANN-GA demonstrated better performance than RSM, achieving optimal power generation values with a lower percentage error when validated against Aspen HYSYS. The power output predicted by ANN-GA was 958.48 kW, exhibiting a minimal error deviation of 0.59% compared to the Hysys-validated output. In contrast, RSM gave an optimal power output of 940.78 kW which gave a percentage error deviation of 1.46%. when validated in HYSYS. These results highlights the superior optimization capabilities of ANN-GA, which effectively integrated machine learning and evolutionary algorithms to achieve higher accuracy in navigating the solution space than RSM.

6. REFERENCES

[1] N.Izuwa, S. Ekwueme, N. Okereke, O.Nwanwe, N. Ohia (2024a) Comparative analysis of geothermal binary ORC systems: performance and environmental considerations for CO2 andwater as geofluids. Zastita Materijala, 65(1), 73-85.

[2] M.Haghghi, Z. Mohammadi, M. Delpisheh, E. Nadimi, H. Athari (2023) Multi-variable study/optimization of a novel geothermal-driven poly-generation system: application of a soft-computing intelligent procedure and MOGWO. Process Safety and Environmental Protection, 171, 507-531.

[3] N.Izuwa, N. Okereke, O. Nwanwe, E. Ejiga, S. Ekwueme, A. Chikwe, C. Ohaegbulam (2024b) Modeling of Wellbore Heat Transfer in Geothermal Production Well. In IOP Conference Series: Earth and Environmental Science, 1342(1), 012041. IOP Publishing.

[4] P.M.B. Abrasaldo, S.J. Zarrouk, A.W. Kempa-Liehr (2024) A systematic review of data analytics applications in above-ground geothermal energy operations. Renewable and Sustainable Energy Reviews, 189, 113998.

[5] N. C. Izuwa, V. E. Udigwe, O. I. Nwanwe, N. U. Okereke (2022) Investigation of the Potentials of Heat Extraction from Abandoned Oil Wells for Electricity Generation. Petroleum & Coal, 64(4).

[6] C. Temizel, U. Odi, C. Cetin, Y. Pamukcu, C. Yegin (2024, April) Challenges and Recent Advances in Modeling and Simulation of Geothermal Systems. In SPE Western Regional Meeting, p. D021S010R006. SPE.

[7] Z. Said, P. Sharma, A. K. Tiwari, Z. Huang, V. G. Bui, A. T. Hoang (2022) Application of novel framework based on ensemble boosted regression trees and Gaussian process regression in modelling thermal performance of small-scale Organic Rankine Cycle (ORC) using hybrid nanofluid. Journal of Cleaner Production, 360, 132194.

[8] J. Oyekale, B. Oreko (2023) Machine learning for design and optimization of organic Rankine cycle plants: A review of current status and future perspectives. Wiley Interdisciplinary Reviews: Energy and Environment, 12(4), e474.

[9] S. Ramachandran, S. S. Bhogilla, P. K. Vijayan (2024) Techno-economic analysis and optimization of a binary geothermal combined district heat and power plant for Puga Valley, India. Renewable Energy, 234, 121223.

[10] A. G. Sangesaraki, A. Gharehghani, J. R. Mehrenjani (2023) 4E analysis and machine learning optimization of a geothermal-based system integrated with ejector refrigeration cycle for efficient hydrogen production and liquefaction. International Journal of Hydrogen Energy, 48(82), 31875–31904.

[11] J. Xie, J. Wang (2022) Compatibility investigation and techno-economic performance optimization of whole geothermal power generation system. Applied Energy, 328, 120165.

[12] P. Ding, K. Zhang, Z. Yuan, Z. Wang, D. Li, T. Chen, … R. Shofahaei (2021) Multi-objective optimization and exergoeconomic analysis of geothermal-based electricity and cooling system using zeotropic mixtures as the working fluid. Journal of Cleaner Production, 294, 126237.

[13] R. DiPippo (2024) Extraction turbines and feed-heating in geothermal binary plants: A thermodynamic performance assessment. Geothermics, 116, 102857.

[14] M. A. Haghghi, Z. Mohammadi, M. Delpisheh, E. Nadimi, H. Athari (2023) Multi-variable study/optimization of a novel geothermal-driven poly-generation system: application of a soft-computing intelligent procedure and MOGWO. Process Safety and Environmental Protection, 171, 507–531.

[15] D. Pan, S. G. Farkoush (2023) Comprehensive analysis and multi-objective optimization of power and cooling production system based on a flash-binary geothermal system. Applied Thermal Engineering, 229, 120398.

[16] T. Parikhani, M. Delpisheh, M. A. Haghghi, S. G. Holagh, H. Athari (2021) Performance enhancement and multi-objective optimization of a double-flash binary geothermal power plant. Energy Nexus, 2, 100012.

[17] E. R. Khama, E. Z. Loyibo, W. Okologume, S. T. Ekwueme, C. V. Okafor, N. P. Ohia (2024) Investigation of the performance of activated carbon derived from ripe plantain peels for CO_2 capture: Modelling and optimisation using response surface methodology. Zastita Materijala, 65(2), 258–272.

[18] M. Assareh, P. Yavari, M. Jamil, B. Rafiei, E. Assareh (2024) Thermodynamic analysis of a multiple energy production system based on geothermal energy for commissioning in Canada and optimization by response surface method (RSM). Energy, 302, 131669.

[19] A. Haghighi, M. R. Pakatchian, M. E. H. Assad, V. N. Duy, M. Alhuyi Nazari (2021) A review on geothermal Organic Rankine cycles: modeling and optimization. Journal of Thermal Analysis and Calorimetry, 144, 1799–1814.

[20] A. M. Al Jubori, R. Al-Dadah, S. Mahmoud (2017) Performance enhancement of a small-scale organic Rankine cycle radial-inflow turbine through multi-objective optimization algorithm. Energy, 131, 297–311.

[21] M. E. Kazemian, S. G. Nassab, E. J. Javaran (2022) Comparative techno-economic investigation of CCHP combined by GSHP based on response surface methodology. Thermal Science and Engineering Progress, 34, 101386.

[22] S. Azizi, H. Shakibi, A. Shokri, A. Chitsaz, M. Yari (2023) Multi-aspect analysis and RSM-based optimization of a novel dual-source electricity and cooling cogeneration system. Applied Energy, 332, 120487.

[23] Z. Xue, S. Yao, H. Ma, C. Zhang, K. Zhang, Z. Chen (2023) Thermo-economic optimization of an enhanced geothermal system (EGS) based on machine learning and differential evolution algorithms. Fuel, 340, 127569.

[24] E. Assareh, S. Hoseinzadeh, N. Agarwal, M. Delpisheh, A. Dezhdar, M. Feyzi, … M. Lee (2023) A transient simulation for a novel solar-geothermal cogeneration system with a selection of heat transfer fluids using thermodynamics analysis and ANN intelligent (AI) modeling. Applied Thermal Engineering, 231, 120698.

[25] A. Tugcu, O. Arslan (2017) Optimization of geothermal energy aided absorption refrigeration system—GAARS: A novel ANN-based approach. Geothermics, 65, 210–221.

[26] D. Ziviani, N. A. James, F. A. Accorsi, J. E. Braun, E. A. Groll (2018) Experimental and numerical analyses of a 5 kWe oil-free open-drive scroll expander for small-scale organic Rankine cycle (ORC) applications. Applied Energy, 230.

[27] C. Yilmaz, I. Koyuncu (2021) Thermoeconomic modeling and artificial neural network optimization of Afyon geothermal power plant. Renewable Energy, 163, 1166–1181.

[28] G. Çetin, O. Özkaraca, A. Keçebaş (2021) Artificial neural network-based optimization of geothermal power plants. In Thermodynamic Analysis and Optimization of Geothermal Power Plants, pp. 263–278. Elsevier.

[29] C. Yilmaz, O. Sen (2022) Thermoeconomic analysis and artificial neural network based genetic algorithm optimization of geothermal and solar energy assisted hydrogen and power generation. International Journal of Hydrogen Energy, 47(37), 16424–16439.

[30] S. Chanthamaly, A. Promwungkwa, K. Ngamsanroaj (2023) Optimal operation of geothermal power plant by artificial neural network.

[31] J. C. Hsieh, Y. C. Li, Y. C. Lin, T. C. Yeh (2024) Off-design performance and economic analysis in coupled binary cycle with geothermal reservoir and turbo-expander. Energy, 305, 132274.

[32] J. Zhou, Y. T. Chu, J. Ren, W. Shen, C. He (2023) Integrating machine learning and mathematical programming for efficient optimization of operating conditions in organic Rankine cycle (ORC) based combined systems. Energy, 281, 128218.

[33] N. Chitgar, A. Hemmati, M. Sadrzadeh (2023) A comparative performance analysis, working fluid selection, and machine learning optimization of ORC systems driven by geothermal energy. Energy Conversion and Management, 286, 117072.

[34] H. Shakibi, M. Y. Faal, E. Assareh, N. Agarwal, M. Yari, S. A. Latifi, … M. Lee (2023) Design and multi-objective optimization of a multi-generation system based on PEM electrolyzer, RO unit, absorption cooling system, and ORC utilizing machine learning approaches; a case study of Australia. Energy, 278, 127796.

[35] W. Ling, Y. Liu, R. Young, T. T. Cladouhos, B. Jafarpour (2024) Efficient data-driven models for prediction and optimization of geothermal power plant operations. Geothermics, 119, 102924.

[36] A. Farajollahi, M. Baharvand, H. R. Takleh (2024) Modeling and optimization of hybrid geothermal-solar energy plant using coupled artificial neural network and genetic algorithm. Process Safety and Environmental Protection, 186, 348–360.

[37] J. Xie, J. Wang (2022) Compatibility investigation and techno-economic performance optimization of whole geothermal power generation system. Applied Energy, 328, 120165.

[38] A. Farajollahi, M. Rostami, M. Feili, H. Ghaebi (2023) Thermodynamic and economic evaluation and optimization of the applicability of integrating an innovative multi-heat recovery with a dual-flash binary geothermal power plant. Clean Technologies and Environmental Policy, 25(5), 1673–1698.

[39] A. A. Mana, S. I. Kaitouni, T. Kousksou, A. Jamil (2023) Enhancing sustainable energy conversion: Comparative study of superheated and recuperative ORC systems for waste heat recovery and geothermal applications, with focus on 4E performance. Energy, 284, 128654.

[40] A. D. P. Putera, A. N. Hidayah, A. Subiantoro (2019) Thermo-economic analysis of a geothermal binary power plant in Indonesia—A pre-feasibility case study of the Wayang Windu site. Energies, 12(22), 4269.

[41] M. Ozturk, I. Dincer (2021) Development of a combined flash and binary geothermal system integrated with hydrogen production for blending into natural gas in daily applications. Energy Conversion and Management, 227, 113501.

[42] H. Ghasemi, M. Paci, A. Tizzanini, A. Mitsos (2013) Modeling and optimization of a binary geothermal power plant. Energy, 50, 412–428.

[43] A. N. Hidayah, A. D. P. Putera, A. Subiantoro (2020, February) Selection of optimum working fluid and cycle configuration of organic Rankine cycle (ORC) as bottoming binary cycle at Wayang Windu geothermal power plant. In Proceedings of the 45th Workshop on Geothermal Reservoir Engineering, Stanford University, California.

[44] G. Buster, P. Siratovich, N. Taverna, M. Rossol, J. Weers, A. Blair, … J. Akerley (2021) A new modeling framework for geothermal operational optimization with machine learning (Gooml). Energies, 14(20), 6852.

[45] A. M. Moustafa, A. S. Shehata, A. I. Shehata, A. A. Hanafy (2022) Reuse of abandoned oil and

gas wells for power generation in Western Desert and Gulf of Suez fields of Egypt. Energy Reports, 8, 1349–1360.

[46] M. T. Islam, M. N. Nabi, M. A. Arefin, K. Mostakim, F. Rashid, N. M. S. Hassan, … S. M. Muyeen (2022) Trends and prospects of geothermal energy as an alternative source of power: A comprehensive review. Heliyon, 8(12).

[47] H. D. V. Venomhata, P. O. Oketch, B. B. Gathitu, P. Chisale (2023) Working fluid selection for the geothermal-solar hybrid cycle at Olkaria II power plant in Kenya. Heliyon, 9(1).

[48] Z. Zeng, Y. Chen, C. Li, Y. Li, X. Wu (2021) Parametric analysis and system optimization of a novel steam production system by synthetic cascade utilization of industrial waste heat. Energy Reports, 7, 5909–5921.

[49] P. H. Niknam, L. Talluri, D. Fiaschi, G. Manfrida (2021) Sensitivity analysis and dynamic modelling of the reinjection process in a binary cycle geothermal power plant of Larderello area. Energy, 214, 118869.

[50] P. Ziółkowski, R. Hyrzyński, M. Lemański, B. Kraszewski, S. Bykuć, S. Głuch, … J. Badur (2021) Different design aspects of an Organic Rankine Cycle turbine for electricity production using a geothermal binary power plant. Energy Conversion and Management, 246, 114672.

[51] S. N. Karlsdottir, H. Pálsson, A. Manadao Bravo Jr, A. Stefánsson, G. O. Boakye (2023, March) Corrosion Testing of Coatings in Simulated ORC Geothermal Heat Exchanger Environment. In AMPP CORROSION (pp. AMPP-2023). AMPP.

[52] S. Davíðsdóttir, B. G. Gunnarsson, K. B. Kristjánsson, B. A. Ledésert, D. I. Ólafsson (2021) Study of corrosion resistance properties of heat exchanger metals in two different geothermal environments. Geosciences, 11(12), 498.

[53] C. Penot, D. Martelo, S. Paul (2023) Corrosion and scaling in geothermal heat exchangers. Applied Sciences, 13(20), 11549.

[54] C. Tong, C. Tong (2019) Advanced Materials Enable Renewable Geothermal Energy Capture and Generation. In Introduction to Materials for Advanced Energy Systems, pp. 321–377.

[55] F. Fanicchia, S. N. Karlsdottir (2023) Research and development on coatings and paints for geothermal environments: A review. Advanced Materials Technologies, 8(18), 2202031.

[56] A. B. N. Jayakumari, N. G. Malik, G. Mittal, D. Martelo, N. Kale, S. Paul (2023) A review on geothermal heat exchangers: challenges, coating methods, and coating materials.

[57] M. AlGaiar, J. Afolabi (2024, May) Enhancing Geothermal Wells Integrity: Key Considerations and Challenges from Drilling to Production. In SPE Symposium: Well Integrity Management, p. D021S005R001. SPE.

[58] O. Jiang, L. Cao, W. Zhu, X. Zheng (2024) Review of Reservoir Damage Mechanisms Induced by Working Fluids and the Design Principles of Reservoir Protection Fluids: From Oil–Gas Reservoirs to Geothermal Reservoirs. Energies, 17(19), 4895.

[59] W. Kibikas, C. Chang, S. J. Bauer, S. Nakagawa, P.Dobson, T. Kneafsey, A. Samuel (2024) Time-dependent thermal degradation of lost circulation materials in geothermal systems. Geothermics, 121, 103038.

[60] B. Meng, G. Yan, P. He, Q. Zhou, W. Xu, Y. Qiao (2025) Nanotechnology applications in geothermal energy systems: Advances, challenges and opportunities. Advances in Geo-Energy Research, 15(2), 172–180.

[61] N. Olry, A. Cascone, M. Eils, L. Bussaglia, V. Smith (2024) Geothermal Drilling Fluid Meets Performance, Environmental, and Regulatory Challenges in the Alps. In Proceedings of the 2024 AADE Fluids Technical Conference and Exhibition. American Association of Drilling Engineers.

[62] S. Paul, C. Leahy (2024, March) Performance of Damaged Thermal Spray Coatings in Phase Change Materials (PCMs) Used in Geothermal Plants. In AMPP CORROSION (pp. AMPP-2024). AMPP.

[63] L. Wan, J. Wang, W. Yue, F. Lin, C. Gao, X. Liu, … Z. Huang (2024) Composites with Synergistically Enhanced Thermodynamic and Mechanical Properties for Geothermal Heat Exchangers. Advanced Engineering Materials, 26(22), 2401581.

[64] H. Yunpeng, Z. Mingming, D. Ji, C. Chunrong, L. Junfu, Z. Dongping, … M. Chunchi (2024) Study on the thermo-mechanical properties of adaptive thermal control anchoring materials in high-geothermal tunnels. Construction and Building Materials, 447, 138156.

[65] Q. Zhang, Y. Q. Feng, K. J. Xu, H. J. Liang, Z. N. Liu, C. Y. Zhao, C. N. Markides (2024) Dynamic behaviour and performance evaluation of a biomass-fired organic Rankine cycle combined heat and power (ORC-CHP) system under different control strategies. Applied Thermal Engineering, 248, 123236.

[66] J. Wu, Y. Liang, Z. Sun, Y. Zhu, J. Ye, J. Lu (2024) Dynamic analysis and control strategy of ORC coupled ejector expansion refrigeration cycle driven by geothermal water. Journal of Cleaner Production, 445, 141309.

[67] S. Davoodi, M. Al-Shargabi, D. A. Wood, S. Slivkin, G. Shishaev, V. S. Rukavishnikov (2024) Geothermal energy recovery from abandoned petroleum wells: A review of the challenges and opportunities. Sustainable Energy Technologies and Assessments, 68, 103870.

[68] S. Bilodeau, M. Carty (2024) Conversion of Waste Heat into Electricity Using Combined TESS-ORC Technology. SSRN Paper.

[69] I. Ekeke, C. Mgbemere, C. Nwanze, F. Aniukwu, C. Njoku (2025) Musa paradisiaca stem sap extract as corrosion inhibitor for aluminum protection in acidic environment. Zastita Materijala.

[70] M. H. E. Ahmadi, A. Mosayebi (2021) Fischer–Tropsch synthesis over Co-Ni/Al_2O_3 catalyst: Comparison between comprehensive kinetic modeling, Artificial Neural Network, and a novel hybrid GA-Fuzzy models. Journal of the Taiwan Institute of Chemical Engineers, 127, 32–45.

[71] M. Hojjat, S. G. Etemad, R. Bagheri, J. Thibault (2011) Thermal conductivity of non-Newtonian

nanofluids: experimental data and modeling using neural network. International Journal of Heat and Mass Transfer, 54(5–6), 1017–1023.
[72] E. H. Martinez, M. C. P. Carlos, J. I. C. Solis, M. C. P. Avalos (2020) Thermodynamic simulation and mathematical model for single and double flash cycles of Cerro Prieto geothermal power plants. Geothermics, 83, 101713.
[73] S. Ata, A. Kahraman, R. Şahin (2020) Prediction and sensitivity analysis under different performance indices of R1234ze ORC with Taguchi's multi-objective optimization. Case Studies in Thermal Engineering, 22, 100785.
[74] A. Khosravi, S. Syri, X. Zhao, M. E. H. Assad (2019) An artificial intelligence approach for thermodynamic modeling of geothermal-based organic Rankine cycle equipped with solar system. Geothermics, 80, 138–154.
[75] L. Zhou, Y. Zhang, Z. Hu, Z. Yu, Y. Luo, Y. Lei, … Y. Ma (2019) Analysis of influencing factors of the production performance of an enhanced geothermal system (EGS) with numerical simulation and artificial neural network (ANN). Energy and Buildings, 200, 31–46.

IZVOD

MODELIRANJE I OPTIMIZACIJA GEOTERMALNIH BINARNIH ORC SISTEMA KORIŠĆENJEM METODOLOGIJE POVRŠINE ODGOVORA I VEŠTAČKIH NEURONSKIH MREŽA

Ova studija se fokusira na modeliranje i optimizaciju geotermalnih binarnih sistema Organic Rankine Cicle (ORC) kako bi se poboljšala proizvodnja energije iz geotermalnih sistema koji koriste vodu kao geofluid. Aspen HISIS, koji koristi Peng-Robinsonov paket svojstava, korišćen je za simulaciju procesa, generišući kritične podatke procesa za naknadno modeliranje i optimizaciju. Metodologija površine odgovora (RSM) i veštačka neuronska mreža (ANN) su korišćene za modeliranje odnosa između ulaznih faktora i izlaznog odgovora, koristeći Bok-Behnken dizajn (BBD) za tri ključne ulazne varijable: brzinu protoka radnog fluida, izlazni pritisak radnog fluida i izlazni pritisak turbine. I RSM i ANN su pokazali snažne prediktivne sposobnosti, pri čemu je RSM postigao R2 vrednost od 0,9966 i RMSE od 12,254, dok je ANN postigao R2 vrednost od 0,9886 i RMSE od 23,722, što ukazuje da je RSM neznatno nadmašio ANNccura u smislu ANNccura. Optimizacija ORC sistema je sprovedena korišćenjem RSM i ANN u kombinaciji sa genetskim algoritmom (ANN-GA), sa ciljem određivanja optimalnih vrednosti za ulazne i izlazne parametre. Rezultati optimizacije ANN-GA su potvrđeni korišćenjem Aspen HISIS i pokazali su superiorne performanse u odnosu na RSM. ANN-GA je predvideo optimalne vrednosti protoka radnog fluida, izlaznog pritiska radnog fluida i izlaznog pritiska iz turbine od 12 kg/s, 19 bara i 1,2 bara, respektivno, što je savršeno odgovaralo rezultatima validacije Aspen HISIS. Ova optimizacija je dala izlaznu snagu od 958,48 kV, koja je bila usko usklađena sa izlazom validacije Aspen HISIS od 952,9 kV, što odražava minimalnu procentualnu grešku od 0,59%. Nasuprot tome, RSM je predvideo blago odstupanje optimalnih vrednosti od 11,8 kg/s, 18,47 bara i 1,2 bara, sa odgovarajućom izlaznom snagom od 940,78 kV. Kada je potvrđen sa HISIS-om, RSM-predviđena izlazna snaga je bila 927,2 kV, što je rezultiralo većom greškom u procentima od 1,46%, čime je lošiji učinak u odnosu na ANN-GA. Studija naglašava komparativne snage RSM-a i ANN-GA, pokazujući da, dok se RSM ističe u preciznom modeliranju odnosa i interakcija između ulaznih faktora i izlaznih odgovora, ANN-GA okvir pokazuje znatno veću sposobnost u navigaciji složenim nelinearnim optimizacijskim pejzažima. Ovo naglašava efikasnost integracije modela mašinskog učenja sa metaheurističkim algoritmima za poboljšane performanse optimizacije. Nalazi doprinose unapređenju metodologije za optimizaciju geotermalnih ORC sistema i nude robustan okvir za poboljšanje efikasnosti proizvodnje energije u primenama geotermalne energije.

Ključne reči: *Geotermalna energija, RSM, ANN, genetski algoritam, Hisis simulacija, Proizvodnja električne energije, binarni ORC sistemi*

Naučni rad
Rad primljen: 25.12.2024.
Rad korigovan: 30.04.2025.
Rad prihvaćen: 09.06.2025.

Ubanozie Julian Obibuike https://orcid.org/0000-0003-1382-9160
Stanley ToochukwuEkwueme https://orcid.org/0000-0003-3446-0905
NnaemekaPrincewillOhia https://orcid.org/0000-0002-4219-7062
Frank ChineduUkaeru Nil
Michael IfeanyiOnyejekwe https://orcid.org/0000-0001-6489-6801